European Journal of Pharmacology 614 (2009) 22–29

Contents lists available at ScienceDirect

European Journal of Pharmacology

journal homepage: www.elsevier.com/locate/ejphar

Molecular and Cellular Pharmacology

Functional and molecular characterizations of chloride channels in rat pleural mesothelial cells

Yuya Yoshise, Koichi Ito, Hirokazu Tsubone, Masayoshi Kuwahara *

Department of Comparative Pathophysiology, Graduate School of Agricultural and Life Sciences, The University of Tokyo, 1-1-1 Yayoi, Bunkyo-ku, Tokyo 113-8657, Japan

ARTICLE INFO

Article history:
Received 2 March 2009
Received in revised form 27 April 2009
Accepted 7 May 2009
Available online 14 May 2009

Keywords:
Cl^- channels
ClC-3
Mesothelial cells

ABSTRACT

The purposes of the present study were to clarify whether some Cl^- channels exist in rat pleural mesothelial cells, and to investigate functional and molecular characteristics of these channels. Electrophysiological recordings were performed at room temperature using the whole-cell configuration of the patch-clamp technique. We could observe outwardly rectifying Cl^- currents in rat pleural mesothelial cells under isotonic conditions. These currents exhibited time-dependent inactivation at potential over +60 mV and were inhibited by NPPB. It suggests the presence of voltage-dependent Cl^- channels. Moreover, we observed the currents activated under hypotonic conditions. Their biophysical and pharmacological properties exhibited as follows; moderate outward rectification of whole-cell currents; time-dependent inactivation at large positive potential; anion selectivity with a type-I Eisenman's permeability sequence ($I^->Br^->Cl^->F^->$glutamate$^-$); inhibited by NPPB. These properties are consistent with volume-regulated chloride channels (VRCCs), even though molecular identity of VRCCs could not have been determined, the molecular expressions of mRNA of the Cl^- channels ClC-2, ClC-3, pI_{Cln}, MDR1 were confirmed. The properties of VRCCs in the pleural mesothelial cells were consistent with those of ClC-3 channels, and different from those of ClC-2. Therefore, these results suggest that ClC-3 might contribute to the modulation of VRCCs in rat pleural mesothelial cells.

1. Introduction

Most animal cells have a mechanism for cell volume regulation not only when exposed to either intracellular or extracellular anisomotic conditions but also during cell growth and differentiation, and following the action of external stimuli which generate net fluxes of electrolytes and water (Hoffmann and Simonsen, 1989; Orlov et al., 1992). Animal cells can re-adjust their volume after hypoosmotically induced cell swelling, a mechanism known as regulatory volume decrease (Hoffmann and Simonsen, 1989; Okada and Hazama, 1989; Lang et al., 1998). The regulatory volume decrease occurs through KCl efflux induced by the activation of K^+ and Cl^- channels, and organic osmolytes which is accompanied by obligated loss of water. In addition to volume regulation, volume-regulated chloride channels (VRCCs) have an important role in physiological processes such as cellular metabolism, cell growth, differentiation, migration, and apoptosis. The properties of VRCCs have been well shown in several types of epithelial cells, such as intestinal epithelial cells (Kubo and Okada, 1992). Recent interests were focused on the molecular identity for VRCCs in epithelial cells as well as other cell types. Several proteins have been potential molecular candidates for VRCCs, including P-glycoprotein, pI_{Cln}, ClC-2, and ClC-3. Among these proteins, ClC-3 was proposed to be the protein responsible for VRCCs in human gastric epithelial cells (Jin et al., 2003), bovine epithelial cells (Wang et al., 2000) and vascular smooth muscle cells (Guan et al., 2006). However, some controversy existed about whether ClC-3 mediates volume-sensitive chloride currents (Li et al., 2000; Shimada et al., 2000; Stobrawa et al., 2001; Weylandt et al., 2001).

Because mesothelial cells express the mesenchymal and epithelial cell intermediate filaments (Ferrandez-Izquierdo et al., 1994), mesothelial cells have characteristics very similar to epithelial cells. Mesothelial cells form a sheet on the surface of ever-moving organs (Wang, 1985). This mesothelial layer acts as a biological barrier between the organs and the enveloping serous cavity and has functions involving transport, equilibrium maintenance, and protection. Moreover, mesothelial cells produce cytokines, growth factors, and extracellular matrix constituents (Kuwahara and Kagan, 1995). In turn, mesothelial cells respond to some agents including cytokines and growth factors (Boylan et al., 1992; Hott et al., 1992; Ito et al., 1995; Kuwahara and Kuwahara, 1998; Owens and Grisham, 1993). However, there are only a few data about Cl^- channels in mesothelial cells to date. Therefore, the aims of this study were (1) to clarify whether some Cl^- channels exist in rat pleural mesothelial cells, and (2) to investigate the functional and molecular characteristics of these channels.

* Corresponding author. Tel./fax: +81 3 5841 5391.
E-mail address: akuwam@mail.ecc.u-tokyo.ac.jp (M. Kuwahara).

0014-2999/$ – see front matter © 2009 Elsevier B.V. All rights reserved.
doi:10.1016/j.ejphar.2009.05.001

2. Materials and methods

Adult male Wistar rats (7 to 8 weeks old 200–250 g) were purchased from Saitama Experimental Animals Supply Co., Ltd. (Saitama, Japan). All experiments were performed in accordance with the Institute of Ethical Guidelines under the protocols approved by the Animal Experimental Expert Committee of the University of Tokyo, which are consistent with the Guide for the Care and Use of Laboratory Animals published by the United States National Institutes of Health.

2.1. Cell culture

Rat pleural mesothelial cells were obtained and established in culture, as described previously (Kuwahara et al., 1991). Briefly, adult Wistar rats were anesthetized with sodium pentobarbital (40 mg/kg i.p.) and were immediately killed by exsanguinations from a severed abdominal aorta. The complete thoracic wall was removed under sterile conditions and immersed in petri dishes for 20 min in Hanks' balanced salt solution (HBSS). The parietal pleural surfaces were scraped repeatedly with cell scrapers. The cells were then seeded into culture dishes. The cultures were maintained for up to 10 passages in Dulbecco's modified eagles medium (DMEM) with 10% fetal bovine serum, 10^5 U/l penicillin, and 100 mg/l streptomycin, at 37 °C in a humidified environment containing 5% CO_2. The cultured cells exhibited the characteristic features of mesothelial cells: a polyhedral, cobblestone morphologic pattern and positive immunohistochemical staining for cytoleratin and vimentin (Kuwahara et al., 1991).

2.2. Electrophysiological recording

Experiments were performed at room temperature using the whole-cell configuration of the patch-clamp technique. Before the experiment, rat pleural mesothelial cells grown in sub-confluent cultures were detached by a brief exposure to trypsin and reseed onto coverslips, and used within 24 h. The coverslip was adhered to the bottom of the recording chamber, which was mounted atop an inverted microscope (Olympus, Tokyo, Japan). Patch pipettes were made from borosilicate glass capillaries (O.D. 1.5 mm, I.D. 0.86 mm; Harvard Apparatus, USA) using a two-stage puller (Narishige, Tokyo, Japan), and fire-polished on a microforge. The pipettes had tip resistances of 2–8 MΩ when filled with solution. An Ag–AgCl wire was used as a reference electrode. Liquid junctional potential was calculated using pClamp software (version 8.2; Axon Instruments, Redwood City, CA) and compensated in some experiments. In the experiment of anion substitution, a 3 M KCl agar bridge was used to connect the reference Ag–AgCl electrode. Membrane current was recorded with an Axopatch 200B amplifier (Axon Instruments) using a Digidata 1200 interface (Axon Instruments) and pClamp software. The time courses of current were monitored by repetitively applying (every 15 s) ramp pulses (2-s duration) from the holding potential of 0 mV to test potentials from −100 mV to +40 mV. To observe voltage dependence of the current profile, step pulses were applied from the holding potential of 0 mV to test potential from −100 mV to +60 mV in 20 mV increments. To observe inactivation kinetics at higher membrane potentials, step pulses up to +80 mV were applied. In the experiments for the effects of $[Cl^-]_o$ or anion substitution, reversal potentials (V_{rev}) were measured by applying a ramp pulse (2-s duration) from −40 mV to +40 mV.

Relative anion permeability to Cl^- permeability (P_X/P_{Cl}) was calculated by the Goldman–Hodgkin–Katz equation:

$$P_X / P_{Cl} = \{[Cl^-]_n \exp(-\Delta V_{rev} \times F / RT) - [Cl^-]_s\} / [X^-]_s$$

$[Cl^-]_n$ and $[Cl^-]_s$ are the Cl^- concentrations in the normal and substituted extracellular solutions. $[X^-]_s$ is the concentration of the substituting anion. F is the Faraday constant, R is the gas constant and T is absolute temperature.

2.3. Solutions and drugs

The standard bath solution contained (mM): 113 *N*-methyl-D-glucamine (NMDG), 113 HCl, 30 tetraethylammonium chloride (TEACl), 1.8 $CaCl_2$, 1 $MgCl_2$, 10 2-[4-(2-hydroxyethyl)-1-piperazinyl] ethanesulphonic acid (HEPES), and 5 glucose (pH 7.4 adjusted with NMDG). In some experiments, TEA^+, Ca^{2+} and Mg^{2+} were substituted with $NMDG^+$ and the concentration of Cl^- was changed by replacement with glutamate$^-$. The pipette solution contained (mM): 108 NMDG, 108 HCl, 30 TEACl, 1.9 $CaCl_2$, 4 Mg-ATP, 3 *O,O′*-bis (2-aminoethyl) ethylenglycol-bis-[aminoethylether]-*N,N,N′,N′*-tetraacetic acid (EGTA), 5 glucose, and 10 HEPES (pH 7.2 adjusted with NMDG, free $[Ca^{2+}]_i = 200$ nM).

The isotonic bath solution contained (mM): 90 *N*-methyl-D-glucamine (NMDG), 30 tetraethylammonium chloride (TEACl), 1.8 $CaCl_2$, 1 $MgCl_2$, 10 2-[4-(2-hydroxyethyl)-1-piperazinyl] ethanesulphonic acid (HEPES), 5 glucose and 50 D-mannitol (pH 7.4 adjusted with NMDG). D-mannitol was removed from this solution to make standard hypotonic solution and 100 mM D-mannitol was included to make hypertonic solution. The standard pipette solution contained (mM): 90 NMDG, 90 HCl, 30 TEACl, 1.9 $CaCl_2$, 4 Mg-ATP, 5 *O,O′*-bis (2-aminoethyl) ethylenglycol-bis-[aminoethylether]-*N,N,N′,N′*-tetraacetic acid (EGTA), 10 HEPES and 50 D-mannitol (pH 7.2 adjusted with NMDG, free $[Ca^{2+}]_i = 100$ nM). In the experiments for the effects of $[Cl^-]_o$ and anion substitution, bath solution containing (mM): 120 NMDG, 120 HCl, 1.8 $CaCl_2$, 1 $MgCl_2$, 10 HEPES and 5 glucose (pH 7.4 adjusted with NMDG) was used. The concentration of Cl^- was changed by replacement with glutamate$^-$, and 120 mM Cl^- was replaced by I^-, Br^-, or F^-, respectively. In experiment for the effects of $[Cl^-]_o$, the pipette solution contained (mM): 120 NMDG, 70 HCl, 1.9 $CaCl_2$, 4 Mg-ATP, 5 EGTA, 10 HEPES, 50 glutamate, and 50 D-mannitol (pH 7.2 adjusted with NMDG). 5-nitro-2-(3-phenylpropylamino) benzoic acid (NPPB) was purchased from Sigma Chemical Co. (St. Louis, MO, USA). NPPB was dissolved in dimethyl sulfoxide (DMSO) to make a stock solution and diluted 1000× in the bath solution.

2.4. Isolation of total RNA and RT-PCR

Total RNA was isolated from cultured rat pleural mesothelial cells, which were grown to confluence in 60-mm Petri dishes, using the chaotropic Tizol method followed by Isogen-chloroform extraction and isopropanol precipitation (Chomczynski, 1993). RT reaction was performed with RNA PCR Kit Ver3.0 (Takara Shuzo, Otsu, Japan). Total RNA that had been treated with DNase I was added to the reaction buffer. The final concentration of reaction buffer contained 0.125 μmol hexanucleotide random primers, 50 mM KCl, 5 mM $MgCl_2$, 1 mM of all four dNTPs, 10 mM Tris–HCl (pH = 8.3), 1 U/μl of RNase inhibitor and 0.25 U/μl of AMV reverse transcriptase in 10 μl total reaction volume. The samples were then incubated at 30 °C for 10 min, at 42 °C for 30 min, at 99 °C for 5 min (deactivation of AMV reverse transcriptase), and at 5 °C for 5 min in a thermal cycler (PCR Thermal Cycler PERSONAL, TaKaRa).

In PCR experiments, the earlier published sequences oligonucleotide primers for ClC-2, ClC-3, pICln and MDR1 were used (Abdullaev et al., 2006; Tao et al., 1985; Von Weikersthal et al., 1999; Table 1). The RT reaction products (10 μl) were amplified in the presence of 0.2 μM each of forward and reverse primers 1.25 U of Taq™ polymerase (Takara Shuzo) at a final volume of 50 μl. The samples were preincubated at 94 °C for 10 min. The reaction was set for 35 cycles as follows; denaturation at 94 °C for 1 min, annealing at 60 °C for 1 min and elongation at 72 °C for 1 min.

The 12 μl (with 2 μl of loading buffer) per sample of the PCR products was loaded on 2% agarose gels. The gels were dyed with 1 μg/ml ethidium bromide for 15 min. The molecular weights of the PCR products were compared to a 100-bp molecular weight ladder (Invitrogen). Digitized images of the gels were obtained using a CCD

Table 1
List of sequence-specific primers used for RT-PCR.

Gene product	Forward primer	Reverse primer	Expected length	Refs
ClC-2	CAAGTTCCTCTCCCTCTTTG	GAACTGTCCAAAGCCAGGG	499 bp	Abdullaev et al. (2006)
ClC-3	CCTCTTTCCAAAGTATAGCAC	TTACTGGCATTCATGTCATTTC	552 bp	Abdullaev et al. (2006)
pICln	ATAAGTCAGCATTGGAGGCG	ACTGGCTGCTCACAGACTGA	246 bp	Von Weikersthal et al. (1999)
MDR1	CCCATCATTGCAATAGCAGG	TGTTCAAACTTCTGCTCCTGA	158 bp	Abdullaev et al. (2006)
GAPDH	ATCAAATGGGGTGATGCTGGTGCTG	CAGGTTTCTCCAGGCGGCATGTCAG	505 bp	Tao et al. (1985)

image analyzer (FULA-3000, Fujifilm, Tokyo, Japan) and visualized on Fluro 532 and 580 filters.

2.5. Statistical analysis

Data were given as the mean ± S.E.M of observations (n). Statistical differences of the data were evaluated by Student's paired t test and considered to be significant at $P<0.05$.

3. Results

3.1. Whole-cell currents in rat pleural mesothelial cells

Rat pleural mesothelial cells were voltage clamped in the whole-cell configuration. Whole-cell currents and current–voltage relationship are shown in Fig. 1. Na^+ and K^+ currents were blocked by adding $NMDG^+$ and TEA^+ in the pipette and bathing solutions, and excluding Na^+ and K^+. The whole-cell currents showed time-independent activation between −100 mV and +40 mV, but exhibited time-dependent inactivation over +60 mV (Fig. 1A). Current–voltage relationship was obtained by measuring currents, and exhibited outward rectification (Fig. 1B).

3.2. Effects of external Cl^- ($[Cl^-]_o$) on whole-cell currents in rat pleural mesothelial cells

To examine the effects of $[Cl^-]_o$, the standard bath solutions were replaced with three different concentrations of $[Cl^-]_o$. When $[Cl^-]_o$ was reduced from 148.6 to 35.6 mM, outward currents were reduced, and almost disappeared at 0 mM (Fig. 2A), suggesting that the outward currents were dependent on $[Cl^-]_o$. The reversal potential (V_{rev}) of currents at different concentrations of $[Cl^-]_o$ was obtained from I–V curve (Fig. 2B). When $[Cl^-]_o$ was reduced from 148.6 to 35.6 mM, V_{rev} was shifted to positive potentials [from 0.6 ± 5.3 mV to 33.9 ± 3.1 mV]. These values are approximate to the theoretical E_{Cl} calculated from the Nernst equation ($E_{Cl}=-0.5$ and 36.2 mV, respectively), suggesting that the observed currents were carried almost only by Cl^-. Using the Goldman–Hodgkin–Katz equation, $P_{glutamate}/P_{Cl}$ was evaluated to be 0.05.

3.3. Effect of NPPB on whole-cell currents in rat pleural mesothelial cells

The effect of NPPB was examined on whole-cell currents using voltage steps. The currents were suppressed by NPPB (100 μM) (Fig. 3A). Significant effect of NPPB was observed voltage-independently (Fig. 3B).

3.4. Outwardly rectifying chloride current activated by hypotonic stimulation

After changing from the isotonic solution to the hypotonic solutions, the currents, which were recorded at −100 and +40 mV, increased gradually (Fig. 4). On the other hand, the currents recovered after changing to the hypertonic solutions. The inset of Fig. 4 shows

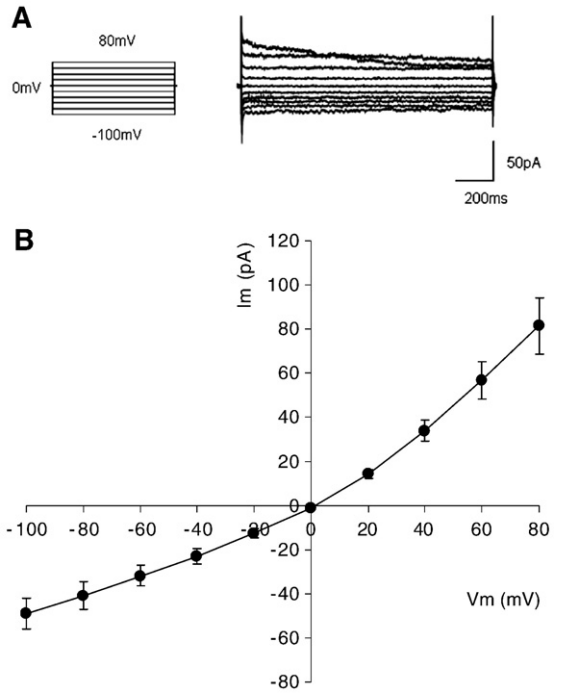

Fig. 1. Whole-cell currents in mesothelial cells. A: Representative current responses to step pulses from −100 mV to +80 mV in 20 mV increments in the standard bath solution. B: Current–voltage relationships of whole-cell currents (mean ± S.E.M., $n=23$).

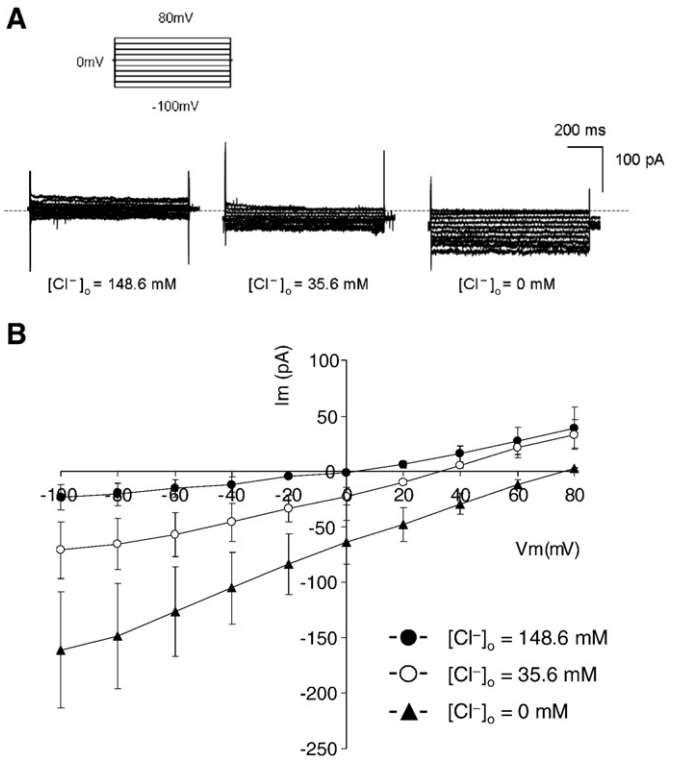

Fig. 2. Effects of $[Cl^-]_o$ on whole-cell currents in mesothelial cells. A: Representative current responses to step pulse from −100 mV to +80 mV in various concentrations of extracellular Cl^-. B: Current–voltage relationships with various concentrations of extracellular Cl^- (mean ± S.E.M., $n=4$).

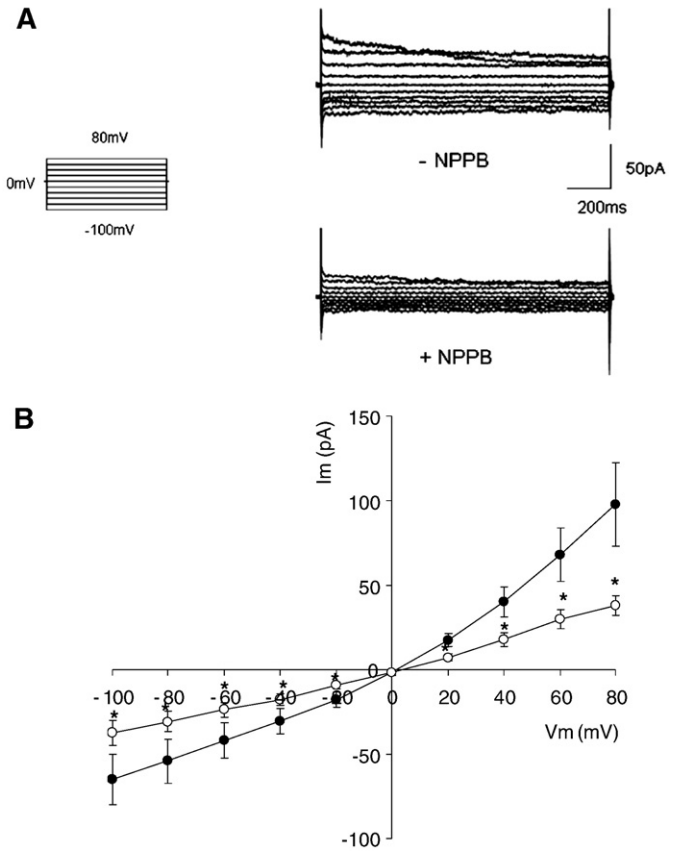

Fig. 3. Effect of 100 μM NPPB on Cl^- currents in mesothelial cells. A: Representative current responses to step pulse from −100 mV to +80 mV in the absence (top) and presence (bottom) of NPPB. B: Current–voltage relationships: ● in the absence and ○ presence of 100 μM NPPB (mean ± S.E.M., $n = 7$).

raw current traces where the arrows indicate the following conditions; (a) isotonic, (b) hypotonic, and (c) hypertonic conditions, respectively. These results clearly showed that the currents were sensitive to extracellular osmolality. Fig. 5A shows raw current traces evoked by step pulses (top) under isotonic (middle) and hypotonic (bottom) conditions. To investigate whether the hypotonicity-induced currents exhibit inactivation at a greater depolarization, step pulses (shown, top) were applied (Fig. 5C). The activated currents exhibited outward rectification (Fig. 5B) and time-dependent inactivation at over +60 mV (Fig. 5C).

3.5. Chloride dependence and anion selectivity

In order to examine the chloride dependence of the activated currents, the reversal potentials (V_{rev}) for the currents were measured using ramp pulses in hypotonic solutions containing four different concentrations of $[Cl^-]_o$, replaced with glutamate$^-$. As shown in Fig. 6, the relation between the $[Cl^-]_o$ and the V_{rev} was linear with a slope of 27 mV/decade, suggesting that the hypoosmotic activated current was induced by the activation of anion channel permeable to Cl^-, although the value was smaller than the theoretical slope (59 mV/decade), which is predicted from the Nernst equation. Using the Goldman–Hodgkin–Katz equation, $P_{glutamate} / P_{Cl}$ was evaluated to be 0.41.

To examine the halide anion selectivity of the activated currents, 120 mM Cl^- in hypotonic solution was replaced with 120 mM I^-, Br^- or F^-. Fig. 7 shows typical raw current traces elicited by voltage ramps applied, and V_{rev} for the currents were measured. The sequence of anion permeability, calculated from the shift of V_{rev}, was $I^- > Br^- > Cl^- > F^-$ (Fig. 6, inset).

3.6. Effect of NPPB

The effect of NPPB was examined on whole-cell currents using voltage steps. The currents activated by hypotonic solutions were

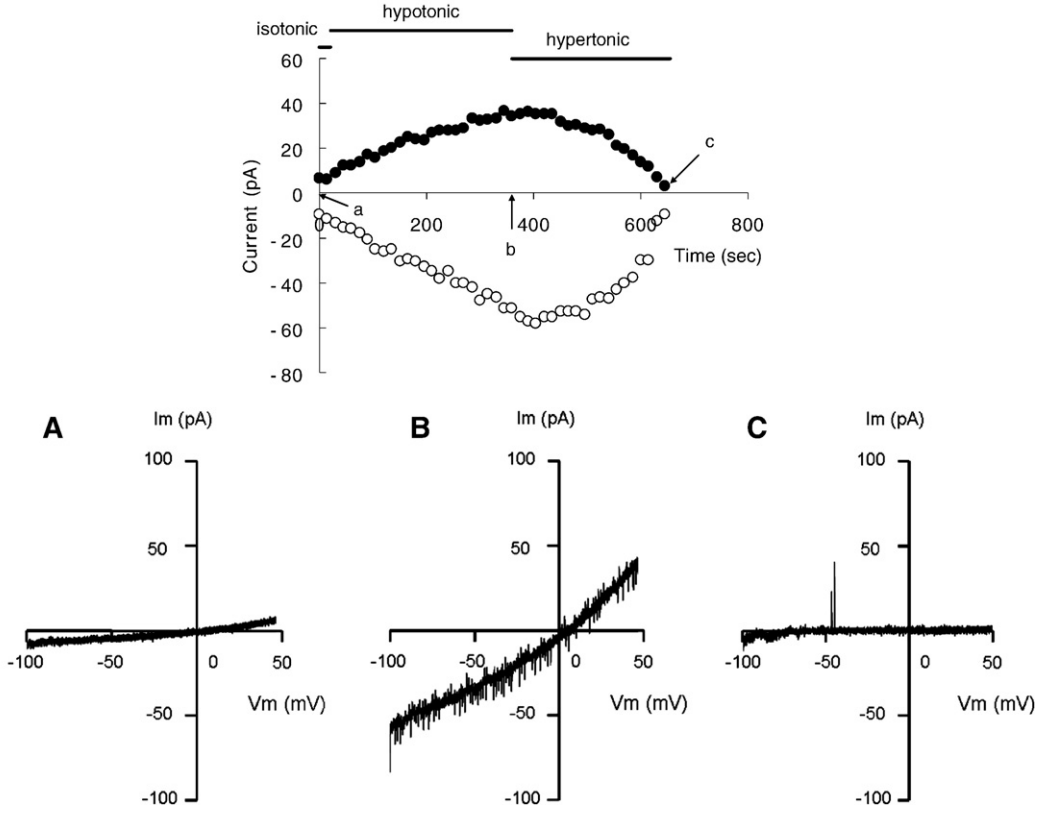

Fig. 4. Activation and recovery of currents induced by osmotic stimulus in rat pleural mesothelial cells. Representative time courses of whole-cell currents at −100 mV (○) and +40 mV (●) in isotonic, hypotonic and hypertonic solutions. Ramp pulses (2-s duration, every 15 s) from −100 mV to +40 mV were applied (inset, raw current trace elicited by ramp pulse at arrows).

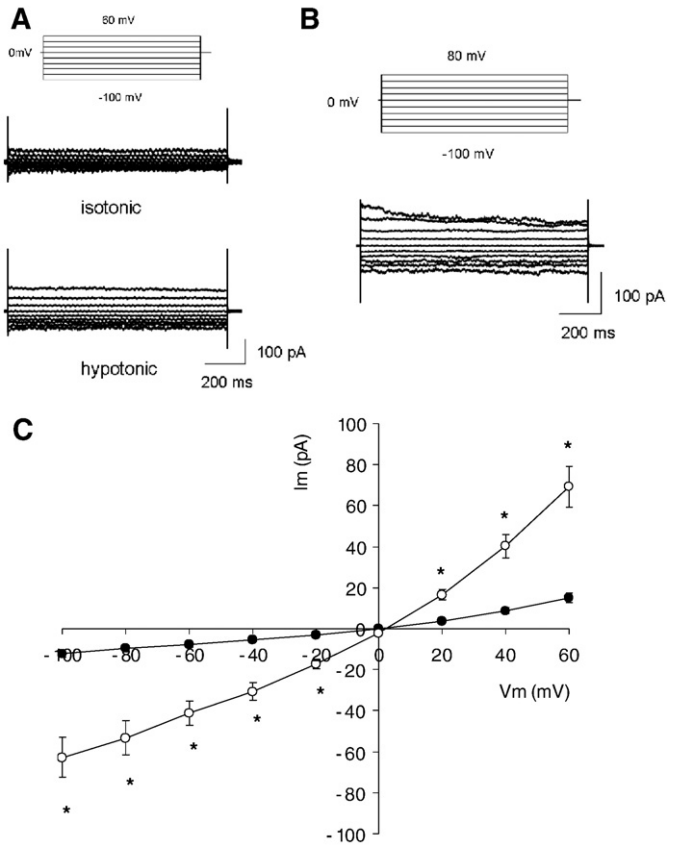

Fig. 5. Whole-cell currents induced by hypotonic solutions in rat pleural mesothelial cells. (A) Representative current elicited by step pulses from −100 mV to +60 mV in isotonic (middle) and hypotonic (bottom) solutions. (B) Representative current elicited by step pulses from −100 mV to +80 mV in hypotonic solution. (C) Current–voltage relationships of whole-cell currents in isotonic (●) and hypotonic solutions (○). Data are shown as mean ± S.E.M., $n = 12$. *P<0.05 vs. isotonic.

suppressed by NPPB (100 μM) (Fig. 8A). Significant effect of NPPB was observed (Fig. 8B).

3.7. Molecular characterization

The RT-PCR technique was used to investigate the molecular expression of mRNA of the chloride channel ClC-2, ClC-3, pI_{Cln}, and MDR1. With primers specific to the rat cDNA sequences of ClC-2, ClC-3, pICln and MDR1, bands corresponding to the expected fragment size, i.e. 499 bp, 552 bp, 246 bp and 158 bp, were obtained from RNA prepared from rat pleural mesothelial cells. As an internal control, we used GAPDH, which gave a band of the expected size of 505 bp. Fig. 9 shows a representative gel of one sample out of three analyzed.

4. Discussion

In the present study, we could observe outwardly rectifying Cl^- currents in rat pleural mesothelial cells under isotonic conditions. These currents exhibited time-dependent inactivation at potential over +60 mV and were inhibited by NPPB. This suggests the presence of voltage-dependent Cl^- channels. Moreover, we observed the currents activated under hypotonic conditions. Their biophysical and pharmacological properties exhibited as follows; (1) moderate outward rectification of whole-cell currents; (2) time-dependent inactivation at large positive potential; (3) anion selectivity with a type-I Eisenman's permeability sequence ($I^- > Br^- > Cl^- > F^- >$ glutamate$^-$); (4) inhibition by NPPB, the conventional chloride channel blocker. These properties are consistent with volume-regulated chloride channels (VRCCs), which have been well described in many cell types (Strange et al., 1996; Nilius et al., 1997; Okada, 1997; Inoue et al., 2005), suggesting the presence of VRCCs in rat pleural mesothelial cells. Even though we were unable to determine the molecular identity of VRCCs, the molecular expressions of mRNA of the Cl^- channels ClC-2, ClC-3, pI_{Cln}, MDR1 were confirmed. The properties of VRCCs in the pleural mesothelial cells were consistent with those of ClC-3 channels, and different from those of ClC-2. Therefore, these results suggest that ClC-3 might contribute to the modulation of VRCCs in rat pleural mesothelial cells.

Outwardly rectifying Cl^- channels were observed in rat pleural mesothelial cells. These currents showed time-dependent inactivation at over +60 mV, and were inhibited significantly by NPPB. Cl^- channels in the cells also were hardly permeable to glutamate, the negatively charged amino acid ($P_{glutamate} / P_{Cl} = 0.05$). These results are similar to the earlier study for Cl^- channels in human pleural mesothelial cells (Meyer et al., 2004). However, NPPB inhibited only about 60% of this currents in rat pleural mesothelial cells, although Meyer et al. (2004) reported that NPPB inhibited the currents about 90%. There is no obvious explanation for the greater propensity of NPPB inhibition in human pleural mesothelial cells, and these differences may simply reflect the species difference of cultured cells, because it is generally thought that the sensitivity to NPPB of Cl^- channels is dependent on different characteristics of cells.

The hypotonicity-induced currents observed in rat pleural mesothelial cells were sensitive to NPPB, the conventional Cl^- channel blocker, but its blockade was observed at a moderate level (Fig. 8).

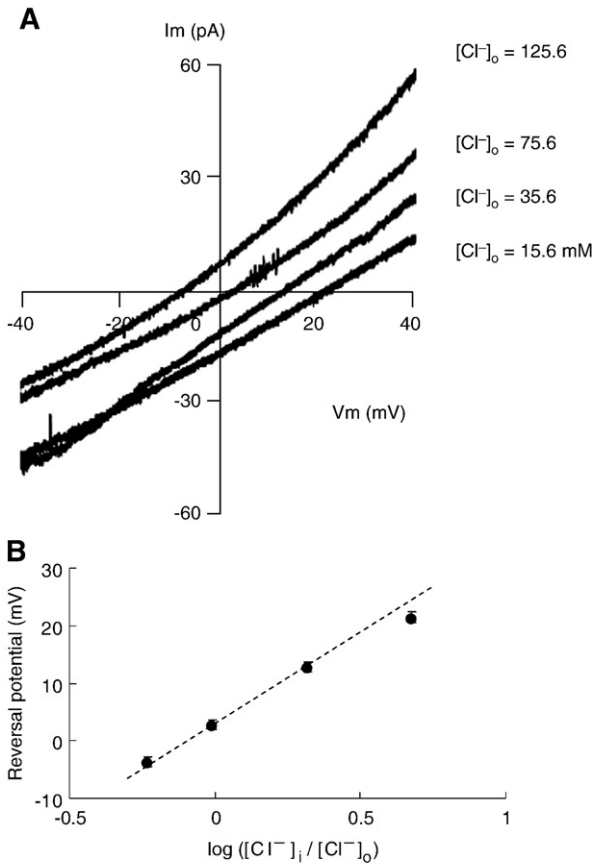

Fig. 6. $[Cl^-]_o$ dependence of volume-sensitive Cl^- channels in rat pleural mesothelial cells. (A) Representative currents resulting from changes in the extracellular Cl concentration ($[Cl^-]_o$). A ramp pulse from −40 mV to +40 mV was applied for 2 s. (B) Relation between the reversal potential (V_{rev}) and $[Cl^-]_o$. Data are shown as mean ± S.E.M., $n = 4$.

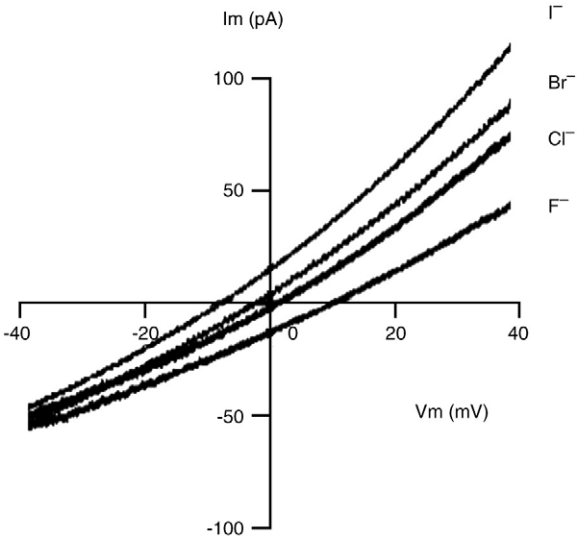

Anion	V_{rev} (mV)	P_x/P_{Cl}	n
I^-	-8.0±0.6	1.44	6
Br^-	-3.3±0.3	1.19	6
Cl^-	1.1±1.2	1	6
F^-	10.5±1.0	0.68	6

Fig. 7. Effects of extracellular anion substitution on volume-sensitive currents in rat pleural mesothelial cells. Cl^- in the bath solution was replaced with I^-, Br^-, or F^-. Representative raw traces elicited by ramp pulse from −40 mV to +40 mV applied for 2 s. Inset shows relative anion permeabilities (P_X / P_{Cl}) calculated by the Goldman–Hodgkin–Katz equation.

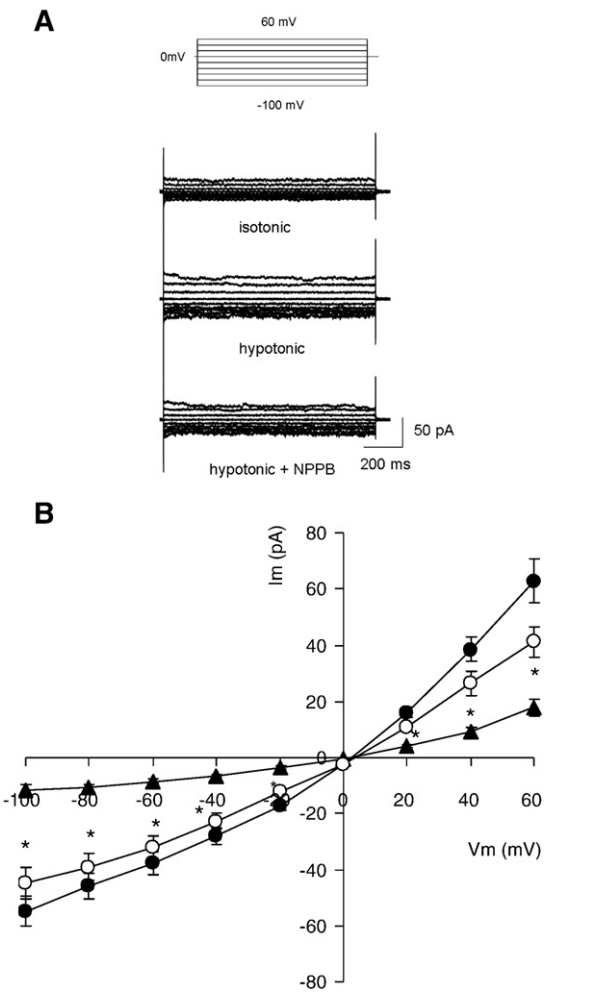

Fig. 8. Effect of 100 μM NPPB on volume-sensitive currents in mesothelial cells. (A) Representative current responses to step pulse from −100 mV to +60 mV in isotonic (top), hypotonic (middle) and hypotonic + NPPB (bottom). (B) Current–voltage relationships; ▲ isotonic, ● hypotonic, ○ hypotonic + NPPB. Data are shown as mean ± S.E.M., $n = 5$. *$P < 0.05$ vs. hypotonic.

The half-maximally effective concentration of NPPB for VRCCs is less than 100 μM in human epithelial cells (Kubo and Okada, 1992). Since mesothelial cells are derived from the mesoderm, but express both mesenchymal and epithelial cell intermediate filaments, mesothelial cells have close similarities to epithelial cells. However, mesothelial cells have voltage-dependent Ca^{2+} channels (Ito et al., 1995), which have not been found in epithelial cells. Therefore, mesothelial cells may have unique characteristics about ion channels. It is considered that properties for VRCCs of mesothelial cells are different from those of epithelial cells. However, further studies will be needed to clarify these issues.

Even though the molecular identity of VRCCs has not been determined, the present study showed that MDR1, pI_{Cln}, ClC-2, and ClC-3 mRNA, which have been candidates for VRACs, were all expressed in rat pleural mesothelial cells. ClC-2 and ClC-3, the ClC family which mediate voltage-dependent channels, are known to be expressed ubiquitously with high mRNA levels (Jentsch et al., 2002). The ClC-2 channel, when expressed, is activated by hypotonicity and hyperpolarization. It shows inward rectification and an anion selectivity of $Cl^- > Br^- > I^-$ (Grunder et al., 1992; Thiemann et al., 1992), which conflict with the obtained results in this study (outward rectification and anion selectivity of $I^- > Br^- > Cl^- > F^-$). Therefore, it seems that ClC-2 did not mainly mediate VRCCs in rat pleural mesothelial cells. Heterologous expression of ClC-3 in NIH/3T3 fibroblasts elicited a volume-sensitive Cl^- current with electrophysiological properties close to native VRCCs (Duan et al., 1997, 1999). Although the properties of VRCCs in rat pleural mesothelial cells are consistent with those of ClC-3 channel, it is unclear whether VRCCs in rat pleural mesothelial cells are mediated by ClC-3, because the role of ClC-3 as a VRCC is still controversial (Stobrawa et al., 2001; Gong et al., 2004). P-glycoprotein is thought to be a regulator of VRCCs (Valverde et al., 1996; Bond et al., 1998) and pI_{Cln} is also thought to regulate VRCCs, however its precise role is still under investigation (Strange, 1998; Eggermont et al., 1998). Our results suggested that ClC-3, including P-glycoprotein and pI_{Cln}, might contribute to the modulation of VRCCs in rat pleural mesothelial cells.

Cl^- channels play important functional roles in diverse processes, such as transportation, blood pressure regulation, cell cycle and apoptosis, muscle tone, synaptic transmission, cellular excitability, cell volume regulation and so on. The mesothelium acts as a biological barrier between the organs and the enveloping serous cavity and

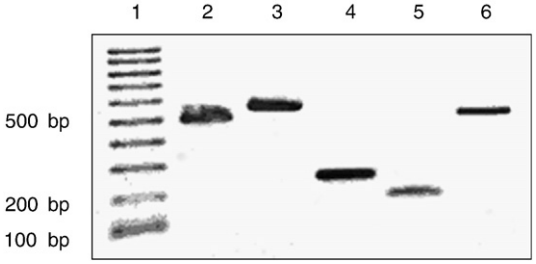

Fig. 9. RT-PCR analysis of ClC-2, ClC-3, pI_{Cln}, MDR1, and GAPDH mRNA expression in rat pleural mesothelial cells. Visible bands correspond to the expected products for; lane 2, ClC-2 (499 bp); lane 3, ClC-3 (552 bp); lane 4, pICln (246 bp); lane 5, MDR1 (158 bp); lane 6, GAPDH (505 bp). Lane 1 contained a 100-bp molecular weight ladder.

has functions involving transport, equilibrium maintenance, and protection. Liquid of the pleural cavity functions as a lubricant as well as a medium to transfer the mechanical actions of the diaphragm and chest wall to the lung, and this system is finely tuned to control pleural fluid volume and turnover (Lai-Fook, 1987; Miserocchi et al., 1991). The pleural mesothelium is a significant barrier to transpleural liquid flow, with permeability of water, small solutes, and proteins. Moreover, it is considered that the osmolarity of pleural fluid changes by pathological condition, such as pleural effusion. Therefore, VRCCs may play key roles in transportation and cell volume regulation in rat pleural mesothelial cells.

In addition to cell volume regulation, VRCCs play important roles in cell proliferation or cell cycle (Shen et al., 2000; Wondergem et al., 2001), migration (Ransom et al., 2001) and cell death (Okada et al., 2006). The mesothelial cell population turns over slowly, renewing with 0.16–0.5% of cells undergoing mitosis at any one time (Mutsaers, 2004), with proliferation balanced by cell death. Injury to the mesothelium triggers events leading to the migration of mesothelial cells from the edge of the lesion towards the wound center and desquamation of cells into the serosal fluid which attach and incorporate into the regenerating mesothelium (Mutsaers, 2004). Therefore, VRCCs in pleural mesothelial cells may be involved with these functions.

The present study could successfully show the electrophysiological data of Cl^- channels in rat pleural mesothelial cells for the first time. Although it is suggested that rat pleural mesothelial cells may express various ion channels, such as voltage-gated Ca^{2+} channels (Ito et al., 1995), receptor-operated Ca^{2+} channels (Kuwahara and Kuwahara, 2002), and store-operated Ca^{2+} channel (Kuwahara and Kuwahara, 2006), electrophysiological studies have not been performed yet. Therefore, the present patch-clamp techniques may become a powerful tool to investigate Cl^- channels as well as other ion channels in rat pleural mesothelial cells.

In conclusion, this study has shown that rat pleural mesothelial cells have Cl^- channels, which share many characteristics of VRCCs described in other cells. Therefore, VRCCs in rat pleural mesothelial cells may play important physiological and pathophysiological roles in the pleural cavity.

References

Abdullaev, I.F., Rudkouskaya, A., Schools, G.P., Kimelberg, H.K., Mongin, A.A., 2006. Pharmacological comparison of swelling-activated excitatory amino acid release and Cl^- currents in cultured rat astrocytes. J. Physiol. 572, 677–689.

Bond, T.D., Higgins, C.F., Valverde, M.A., 1998. P-glycoprotein and swelling-activated chloride channels. Methods Enzymol. 292, 359–370.

Boylan, A.M., Ruegg, C., Kim, K.J., Hebert, C.A., Hoeffel, J.M., Pytela, R., Sheppard, D., Goldstein, I.M., Broaddus, V.C., 1992. Evidence of role for mesothelial cell-derived interleukin 8 in the pathogenesis of asbestos-induced pleurisy in rabbits. J. Clin. Invest. 89, 1257–1267.

Chomczynski, P., 1993. A reagent for the single-step simultaneous isolation of RNA, DNA and proteins from cell and tissue samples. Biotechniques 15, 532–537.

Duan, D., Winter, C., Cowley, S., Hume, J.R., Horowitz, B., 1997. Molecular-identification of a volume-regulated chloride channel. Nature 390, 417–421.

Duan, D., Cowley, S., Horowitz, B., Hume, J.R., 1999. A serine residue in ClC-3 links phosphorylation–dephosphorylation to chloride channel regulation by cell volume. J. Gen. Physiol. 113, 57–70.

Eggermont, J., Buyse, G., Voets, T., Tytgat, J., Droogmans, G., Nilius, B., 1998. Is there a link between protein pICln and volume-regulated anion channels? Biochem. J. 331, 347–349.

Ferrandez-Izquierdo, A., Navarro-Fos, S., Gonzalez-Devesa, M., Gil-Benso, R., Llombart-Bosch, A., 1994. Immunocytochemical typification of mesothelial cells in effusions: in vivo and in vitro models. Diagn. Cytopathol. 10, 256–262.

Gong, W., Xu, H., Shimizu, T., Morishima, S., Tanabe, S., Tachibe, T., Uchida, S., Sasaki, S., Okada, Y., 2004. ClC-3-independent, PKC-dependent activity of volume-sensitive Cl channel in mouse ventricular cardiomyocytes. Cell. Physiol. Biochem. 14, 213–224.

Grunder, S., Thiemann, A., Pusch, M., Jentsh, T.J., 1992. Regions involved in the opening of ClC-2 chloride channel by voltage and cell volume. Nature 360, 759–762.

Guan, Y.Y., Wang, G.L., Zhou, J.G., 2006. The ClC-3 Cl^- channel in cell volume regulation, proliferation and apoptosis in vascular smooth muscle cells. Trends Pharmacol. Sci. 27, 290–296.

Hoffmann, E.K., Simonsen, L.O., 1989. Membrane mechanisms in volume and pH regulation in vertebrate cells. Physiol. Rev. 69, 315–382.

Hott, J.W., Spatks, J.A., Godbey, S.W., Antony, V.B., 1992. Mesothelial cell response to pleural injury: thrombin-induced proliferation and chemotaxis of rat pleural mesothelial cell. Am. J. Respir. Cell. Mol. Biol. 6, 421–425.

Inoue, H., Mori, S., Morishima, S., Okada, Y., 2005. Volume-sensitive chloride channels in mouse cortical neurons: characterization and role in volume regulation. Eur. J. Neurosci. 21, 1648–1658.

Ito, K., Kuwahara, M., Sugano, S., Kuwahara, M., 1995. Role of intra- and extracellular calcium stores in mesothelial cell response to histamine. Am. J. Physiol. Lung Cell. Mol. Physiol. 268, L63–L70.

Jentsch, T.J., Stein, V., Weinreich, F., Zdebik, A.A., 2002. Molecular structure and physiological function of chloride channels. Physiol. Rev. 82, 503–568.

Jin, N.G., Kim, J.K., Yang, D.K., Cho, S.J., Kim, J.M., Koh, E.J., Jung, H.C., So, I., Kim, K.W., 2003. Fundamental role of ClC-3 in volume-sensitive Cl^- channel function and cell volume regulation in AGS cells. Am. J. Physiol. Gastrointest. Liver Physiol. 285, G938–G948.

Kubo, M., Okada, Y., 1992. Volume-regulatory Cl^- channel currents in cultured human epithelial cells. J. Physiol. 456, 351–371.

Kuwahara, M., Kagan, E., 1995. The mesothelial cell and its role in asbestos-induced pleural injury. Int. J. Exp. Pathol. 76, 163–170.

Kuwahara, M., Kuwahara, M., 1998. Pericardial mesothelial cells produce endothelin-1 and possess functional endothelin ET_B receptors. Eur. J. Pharmacol. 347, 329–335.

Kuwahara, M., Kuwahara, M., 2002. Involvement of Rho and tyrosine kinase in angiotensin II-induced actin reorganization in mesothelial cells. Eur. J. Pharmacol. 436, 15–21.

Kuwahara, M., Kuwahara, M., 2006. Store-mediated calcium entry in pleural mesothelial cells. Eur. J. Pharmacol. 542, 16–21.

Kuwahara, M., Kuwahara, M., Bijwaard, K.E., Gersten, D.M., Diglio, C.A., Kagan, E., 1991. Mesothelial cells produce a chemoattractant for lung fibroblasts: role of fibronectin. Am. J. Respir. Cell. Mol. Biol. 5, 256–264.

Lai-Fook, S.J., 1987. Mechanics of the pleural space: fundamental concept. Lung 165, 249–267.

Lang, F., Busch, G.L., Ritter, M., Volkl, H., Waldegger, S., Gulbins, E., Haussinger, D., 1998. Functional significance of cell volume regulatory mechanisms. Physiol. Rev. 78, 247–306.

Li, X., Shimada, K., Showalter, L.A., Weinman, S.A., 2000. Biophysical properties of ClC-3 differentiate it from swelling-activated chloride channels in Chinese hamster ovary-K1 cells. J. Biol. Chem. 275, 35994–35998.

Meyer, G., Rodighiero, S., Guizzardi, F., Bazzini, C., Botta, G., Bertocchi, C., Garavaglia, L., Dossena, S., Manfredi, R., Sironi, C., Catania, A., Paulmichl, M., 2004. Volume-regulated Cl^- channels in human pleural mesothelioma cells. FEBS Lett. 559, 45–50.

Miserocchi, G., Negrini, D., Gonano, C., 1991. Parenchymal stress affects interstitial and pleural pressures in in situ lung. J. Appl. Physiol. 71, 1967–1972.

Mutsaers, S.E., 2004. The mesothelial cell. Int. J. Biochem. Cell. Biol. 36, 9–16.

Nilius, B., Eggermont, J., Voet, T., Buyse, G., Manolopoulos, V., Droogmans, G., 1997. Properties of volume-regulated anion channels in mammalian cells. Prog. Biophys. Mol. Biol. 68, 69–119.

Okada, Y., 1997. Volume expansion-sensing outward-rectifier Cl^- channel: fresh start to the molecular identity and volume sensor. Am. J. Physiol. Cell Physiol. 273, C755–C789.

Okada, Y., Hazama, A., 1989. Volume-regulatory ion channels in human epithelial cells. News Physiol. Sci. 4, 238–242.

Okada, Y., Shimizu, T., Maeno, E., Tanabe, S., Wang, X., Takahashi, N., 2006. Volume-sensitive chloride channels involved in apoptotic volume decrease and cell death. J. Membrane Biol. 209, 21–29.

Orlov, S.N., Resink, T.J., Bernhardt, J., Buhler, F.R., 1992. Volume-dependent regulation of sodium and potassium fluxes in cultured vascular smooth muscle cells: dependence on medium osmolality and regulation by signalling systems. J. Membrane Biol. 129, 199–210.

Owens, M.W., Grisham, M.B., 1993. Nitric oxide synthesis by rat pleural mesothelial cells: induction by cytokines and lipopolysaccharide. Am. J. Physiol. Lung Cell. Mol. Physiol. 265, L110–L116.

Ransom, C.B., O'Neal, J.T., Sontheimer, H., 2001. Volume-activated chloride currents contribute to the resting conductance and invasive migration of human glioma cells. J. Neurosci. 21, 7674–7683.

Shen, M.R., Droogmans, G., Eggermont, J., Voets, T., Ellory, J.C., Nilius, B., 2000. Differential expression of volume-regulated anion channels during cell cycle progression of human cervical cancer cells. J. Physiol. 529, 385–394.

Shimada, K., Li, X., Xu, G., Nowak, D.E., Showalter, L.A., Weinman, S.A., 2000. Expression and canalicular localization of two isoforms of the ClC-3 chloride channel from rat hepatocytes. Am. J. Physiol. Gastrointest. Liver Physiol. 279, G268–276.

Strange, K., 1998. Molecular identity of the outwardly rectifying, swelling-activated anion channel: time to reevaluate pICln. J. Gen. Physiol. 111, 617–622.

Strange, K., Emma, F., Jackson, P.S., 1996. Cellular and molecular physiology of volume-sensitive anion channels. Am. J. Physiol. Cell Physiol. 270, C711–C730.

Stobrawa, S.M., Breiderhoff, T., Takamori, S., Engel, D., Schweizer, M., Zdebik, A.A., Bosl, M.R., Ruether, K., Dranguhn, A., Jahn, H., Jentsch, T.J., 2001. Disruption of ClC-3, a chloride channel expressed on synaptic vesicles, leads to a loss of the hippocampus. Neuron 29, 185–196.

Tao, J.Y., Sun, X.H., Kao, T.H., Reece, K.S., Wu, R., 1985. Isolation and characterization of rat and human glyceraldehydes-3-phosphate dehydrogenase cDNAs: genomic complexity and molecular evolution of the gene. Nucleic Acids Res. 13, 2485–2502.

Thiemann, A., Grunder, S., Pusch, M., Jentsch, T.J., 1992. A chloride channel widely expressed in epithelial and non-epithelial cells. Nature 356, 57–60.

Valverde, M.A., Bond, T.D., Hardy, S.P., Taylor, J.C., Higgins, C.F., Altamirano, J., Alvarez-Leefmans, F.J., 1996. The multidrug resistance P-glycoprotein modulates cell regulatory volume decrease. EMBO J. 15, 4460–4468.

Von Weikersthal, S.F., Barrand, M.A., Hladky, S.B., 1999. Functional and molecular characterization of a volume-sensitive chloride current rat brain endothelial cells. J. Physiol. 516, 75–84.

Wang, N.S., 1985. Mesothelial cells in situ. In: Chretien, J., Bignon, J., Hirsch, A. (Eds.), The Pleural in Health and Disease. InDekker, New York, pp. 23–42.

Wang, L., Chen, L., Jacob, T.J., 2000. The role of ClC-3 in volume-activated chloride currents and volume regulation in bovine epithelial cells demonstrated by antisense inhibition. J. Physiol. 524, 63–75.

Weylandt, K.H., Valverde, M.A., Nobles, M., Raguz, S., Amey, J.S., Diaz, M., Nastrucci, C., Higgins, C.F., Sardini, A., 2001. Human ClC-3 is not the swelling-activated chloride channel involved in cell volume regulation. J. Biol. Chem. 276, 17461–17467.

Wondergem, R., Gong, W., Monen, S.H., Dooley, S.N., Gonce, J.L., Conner, T.D., Houser, M., Ecay, T.W., Ferslew, K.E., 2001. Blocking swelling-activated chloride current inhibits mouse liver cell proliferation. J. Physiol. 532, 661–672.